LUNAR POWER TRANSMISSION FOR FISSION SURFACE POWER

Christopher Barth, PhD and David Pike

NASA Glenn Research Center, Cleveland, Ohio, 44135

Primary Author Contact Information: Christopher.b.barth@nasa.gov, 216-433-2678

This work reviews key considerations and challenges in the implementation of lunar power transmission for the 40 kW Fission Surface Power (FSP) System. The overall FSP electric power flow is presented, and potential bulk power transmission strategies are discussed. Metallic conductors operating at elevated voltage are identified as the most efficient and feasible solution, and hardware implementation challenges for AC and DC voltage step up/down are discussed. This work is intended to drive progress on identifying the most feasible power transmission strategy for landed fission power and does not represent consensus or preference by NASA regarding a particular course of action.

I. Application and Challenges

The current Fission Surface Power (FSP) program is focused on developing a landed-lunar reactor capable of delivering 40 kWe to the user. Current FSP concepts anticipate transferring power 1 to 3 km from the reactor to the user load. Although the distance to the horizon is very dependent on topography, a 3 km separation places the reactor over the 2.4 km lunar horizon from the crew and shields them from radiation.

The cost of lunar payload delivery makes it essential to minimize power system mass. This minimization includes both the power transmission system itself and the added mass of the generation system required to compensate for loses in the transmission. Thus, both the transmission system mass and the specific power of the generation system must be accounted for, and the range of feasible transmission topologies will change based on the specific power density of the source. Current estimates of specific power density for FSP systems are 0.25 kg/W (40 kWe design) to 0.27 kg/W (10 kWe design). This relatively high generation mass demands a high transmission-level efficiency to minimize overall system mass because the mass required to compensate for losses is high [1].

II. FSP Electrical System Architecture

The current government reference design incorporates eight, 6.2 kW Stirling thermal to electric convertors. The free-piston Stirling convertor is a linear machine, and the designs developed in collaboration with NASA have utilized a single-phase linear alternator to convert mechanical energy extracted from thermal energy into electrical energy. During operation Stirling convertors require a controlled load to extract power from the convertor and limit the piston stroke. This is analogous to the operation of a rotary generator driven by a turbine with constant steam flow. The generator must be loaded to prevent overspeed of the generator and turbine. In the case of the steam turbine, the power applied by steam to the turbine can typically be regulated to match generator load. However, the heat applied to the Stirling convertor in space applications is constant (plutonium heat sources) or has a significant control delay (fission heat sources) and thus a controlled load on the Stirling convertor is required.

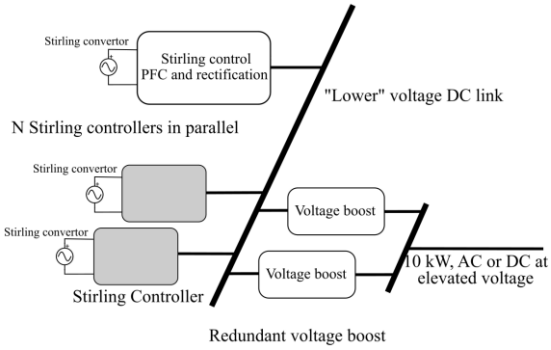

Figure 1: Power architecture for the Stirling-based government reference design (GRD)

The details of Stirling convertor control are a matter of engine design and electrical implementation, but fundamentally the Stirling controller functions as an active power factor correcting rectifier. Instead of operating at unity power factor, as is the goal for most AC-DC rectifiers, the Stirling controller operates with a capacitive phase shift to compensate for the inductance of the Stirling convertor linear alternator and achieves unity power factor with the alternator's ideal back-EMF [2].

The conversion from the Stirling alternator's AC output to the DC link is often questioned as it seems counterproductive in the case of an AC transmission network. This strategy is justified because of the need to maintain a constant load on the Stirling convertor independent of a variable user load. Loading the single-phase alternator while accomplishing power factor correction has been most easily implemented using full power processing and AC-DC rectification. Implementing an AC-AC power conversion strategy would introduce

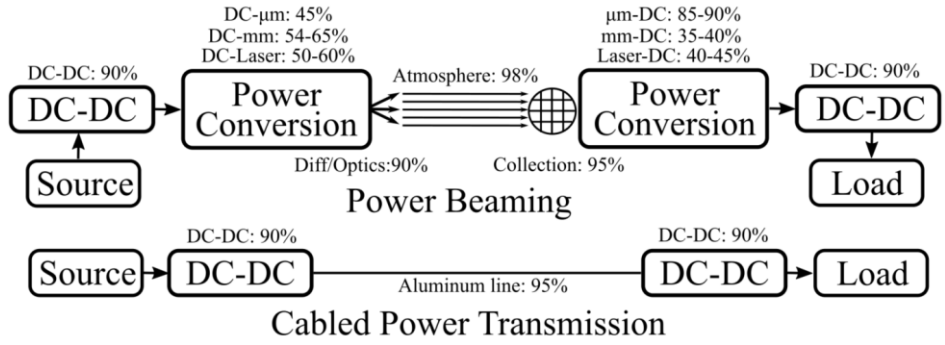

Figure 2: Beamed transmission power flow

extra complexity. Also, Stirling convertors have historically operated at between 50 and 110 Hz, and an AC distribution architecture would be implemented at a higher frequency to reduce mass. Each Stirling convertor is equipped with its own controller, to decouple engine failures and maximize system-level reliability.

The voltage of the DC link will be set by the availability switching and energy buffering technology. The voltage of the Stirling alternators can be traded for current arbitrarily over a relatively wide range with constant efficiency. Aside from the constraints of minimum and maximum wire gauge, the maximum voltage of the alternator is only limited by the decrease in the effective conductive winding area due to the increased volume of non-conducting insulation required at higher voltages. Based on current Stirling convertor implementations and device availability, it is anticipated that the DC link voltage will be between 300 and 400 volts [3] [4]. The conversion of electric power from single-phase AC to DC will require the use of energy buffering capacitors to filter the twice-line-frequency power ripple. On a common DC link, this capacitance will likely be distributed between the Stirling controllers for reliability purposes.

Following the Stirling controllers and the DC link, a redundant voltage boost stage is used to raise the voltage for transmission to minimize both transmission line mass and transmission losses. This voltage boost implementation may be either a DC-DC boost stage or a DC-AC inverter with a voltage boost transformer. In addition to high voltage cables, other strategies such as superconducting cable and power beaming are discussed in following sections.

As system generation capacity increases, Brayton generation systems achieve higher specific power density (kw/kg) than Stirling convertors. Prior demonstrations of Brayton systems for fission power have incorporated 3-phase generator operating at 0.8 kHz to 1.6 kHz [5] [6] [7] [8] [9]. Under this configuration it would be possible to transmit 3-phase power directly from the Brayton generator. However, power from the Brayton system could also be rectified and converted for transmission. Additional analysis is in process at GRC to determine the most effective power transmission strategy.

III. Power Transmission Strategies

Continuous point-to-point power transfer can be accomplished using electro-magnetic wave beaming or conductive cable strategies. Each strategy includes several optimizations that can be considered such as EM wave frequency, conductor material, and DC current vs. AC current at a range of frequencies.

III.A. Power Beaming

Power beaming is by far the least technologically mature strategy for lunar power transfer but attracts significant interest due to its novelty and potential for simplified, long-distance power transfer. Understanding the proper use case for beaming technology is critical for effective planning.

Figure 2 compares the power flow and efficiencies from published literature for a wired system with that of beamed power transfer at three different wavelength classes [10] [11] [12] [13] [14] [15]. Microwave class (2-35 GHz) waves result in large, relatively efficient systems over short distances where beam spread is less significant. Millimeter class waves hold potential as a compromise between size and efficiency but need significant development. Laser-based systems are beneficial where system size needs to be minimized and over long distances where beam spread is an issue. A cabled system provides the most direct form of power transfer; however, the cable has mass and limits the movement of the system. It is clear from these values that the use of power beaming for bulk power transfer in the FSP system would increase the system mass by an order of magnitude or more compared to a cabled power system.

Table 1 explores the mass penalty incurred in the need to increase generation capacity to compensate for the power loss in each transmission strategy. This analysis assumes a linear specific mass of the FSP system. These figures neglect the mass of the transmission system and only account for the added power generation capacity

required to compensate for losses. The mass of the power beaming or cable system would be in addition to the listed mass gain. It is clear from these values that the use of power beaming for bulk power transfer in the FSP system would increase the system mass by an order of magnitude or more compared to a cabled power system.

Table 1: Mass impact of transmission losses for 40 kW FSP system assuming a specific mass of 270 kg/kW [16] [10].

Form	Efficiency	Additional Generation (kWe)	Mass gain (kg)
µm	26%-27%	110	30,000
mm	13%-18%	220	60,000
Laser	14%-18%	210	57,000
HV Line	77%	12	3,200

Relatively few power beaming demonstrations have been conducted at significant power levels. The Power Transmitted over Laser (PTROL) Navy beaming in 2019 demonstrated an efficiency of 20% transmitting 400 W over 330 meters. The unoptimized transmission and receiving system had a mass of >2500 kg. For a 40 kW FSP system this power beaming system and the generation capacity required to compensate for losses is over 10 times heavier than the mass of a cable with voltage boost and buck and accompanying generation capacity. This demonstrates that power beaming is not optimal for bulk power transfer from a fission source [17].

It should be noted that power beaming offers both mass and flexibility benefits in low power, long distance power transfer and applications in which the generation source has a high specific power. This is because EM waves travel unhindered through free space while line mass and losses add linearly with cable length. So, although power beaming is not mass competitive for bulk power transfer from a relatively heavy landed fission system, it should be investigated further for mobile user loads such as small rovers or for high specific power energy sources such as orbiting photovoltaic panels.

III.B. Super Conducting Cables

Superconducting power systems offer virtually lossless power transmission without the need for voltage conversion at transmission. This comes with the caveat that the conductors must be kept cold. The vacuum and low ambient temperature of the lunar night raise the possibility of superconducting power transfer on the moon, but closer investigation demonstrates infeasibility.

A cryogenic coolant system would be required for any superconducting power system on the moon which will experience the lunar day, as daytime temperatures can reach upwards of 400K. Even an optimally routed cable near the lunar pole, which receives less direct sunlight during the day than the equator, cannot avoid regions that will see temperatures which exceed 220K. A superconducting power transmission system would require a superconductor, a cryogenic coolant such as liquid nitrogen, hoses for the coolant, cryocoolers and pumping systems to maintain low coolant temperatures, and radiator systems for those cryocoolers. The superconductor itself is very light; commercially available superconductors weigh only a few kilograms per kilometer. However, issues become clear when the other components of a cryogenic power system are evaluated.

Commercially available stainless-steel hoses with inner diameters of .5 in weigh at least .25 kg/m. Hoses would need to be run in each direction for a complete circuit for the coolant, so 2 km of hoses would be required for 1 km of power transmission. The overall hose mass would be at least 500 kg for a 1 km system. The volume of liquid nitrogen required to fill these hoses would be approximately 250 L. This equates to a mass of approximately 200 kg of liquid nitrogen. Cryocoolers offer heat removal at a rate of approximately 1W/kg [18]. With a hose length of 2 km, and a heat leak rate of 0.92 W/m [19], the cryocoolers would need to remove 1840 W. This much heat means that the cryocoolers' mass would be approximately 1840 kg. The cryocoolers will consume approximately 18.4 kW to create the required 1840 W of lift. A radiator able to dissipate the necessary heat generated by the cryocoolers would be more than 750 kg.

In all, these component masses are over an order of magnitude larger than more traditional cabled systems, making the system prohibitively difficult to deploy. The mass, additional system complexity, massive power consumption, and relatively unproven technology (compared to simple cables and converters) suggest that a superconducting lunar power transfer is not feasible.

III.C. Carbon Nanotube (CNT) Rope

Carbon nanotube technology has progressed rapidly since its discovery in 1991. This technology promises significant benefits due to its high tensile strength (light weight) as well as good electrical and thermal conductivities at nano scale. Recent progress in the development of CNT rope has opened the possibility of utilizing CNT technology as an electrical conductor.

CNT cables demonstrate nearly indefinite wire fatigue, acid, and corrosion resistance, as well as 4 times the tensile strength of copper. At present, the demonstrated specific conductivity of fabricated CNT cable lags that of copper by as much as 6-10 times. However, unlike copper, CNT has a nearly negligible temperature coefficient of resistivity, meaning that the cable performance holds steady over a wide range of temperatures from 0 C to as high as 400 C. This high temperature stability is advantageous in intermittent applications in which the maximum specific current carrying capability of CNT

(A/kg) exceeds copper because the CNT is capable of withstanding higher losses per kg and resulting higher temperatures than copper.

Current results suggest that the specific conductivity of CNT cables holds significant improvement potential. Recent results on small samples have demonstrated specific conductivity exceeding that of copper with absolute conductivity approaching that of copper [20]. At the time of writing, however, the conductivity of CNT cables does not justify their use in lunar power transfer. For reference, a 10 AWG copper pair is approximately 47 kg/km but an equivalent conductivity CNT cable is estimated at 34 kg/km to 57 kg/km [21] [22]. Thus, immediate lunar power implementation is better served by relying on high TRL metallic conductors. It is likely that CNT may play a role in future spacecraft and implementations of the lunar architecture. Investments in US-based CNT manufacturing capability should be prioritized to enable the US to regain a competitive edge in this technology.

III.D. Metallic Conductors

The use of simple metallic conductors represents the strategy with the lowest program risk for lunar power transfer. Conductors for lunar power transmission could potentially be installed using a variety of strategies including insulated and laid on the surface, suspended from poles, and buried. Although buried and suspended cable would remove the need for full insulation, these strategies rely on lunar infrastructure which is uncertain and would introduce additional programmatic risk. Thus, recent FSP concepts incorporate a fully insulated cable design which is intended to be deployed on the lunar surface.

As mentioned, maintaining transmission system efficiency is critical in the minimization of system-level mass. Over short wire lengths, conduction losses are limited by the need for system efficiency and the heat dissipation capability of the cable. Power transmission for the FSP application is looking at distances of 1 to 3 km, and in this review, cable losses are limited to 5% at 3 km as a design choice. Thus, the power dissipation per length of cable is small for a 40 kW system (0.7 W/m).

With the efficiency of the cable constrained, the required conductor mass decreases with the square of the transmission voltage until the conductor diameter becomes too mechanically fragile to be feasible. In this design, the conductor was maintained larger than 16 AWG. While the conductor mass decreases with voltage, the required insulation mass increases with voltage resulting in a voltage that minimizes overall cable mass.

The design and manufacture of high-voltage, vacuum-rated cables which avoid partial discharge breakdown is an area of ongoing research, however Figure 3 shows an approximate sweep of total cable mass vs DC voltage for the 40 kW, 95% efficient cable described above. The x-axis voltage is provided in terms of voltage of each line with respect to neutral or the FSP lander so that the insulation requirements on each cable are equal and minimized. Fluorinated ethylene propylene (FEP) was assumed at a thickness of 4.4 kV/mm or 5 times the minimum FEP breakdown thickness. Optimal transmission voltage will change depending on the insulation strategy used. This design assumes a 0.6 mm FEP case around the cable assembly but there is no micrometeor shielding or cable redundancy. Figure 3 indicates a DC voltage of about ±4000 VDC or 8000 VDC line-to-line will minimize cable mass under the constraints imposed.

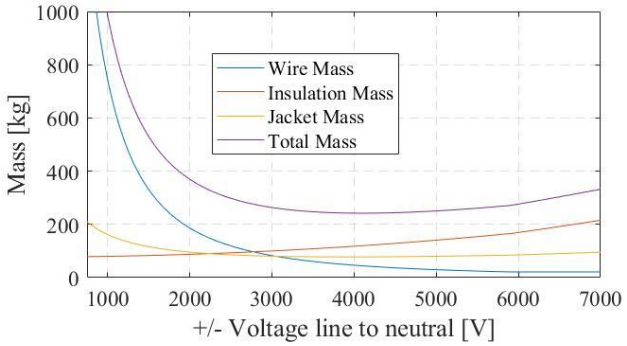

Figure 3: Total mass with breakdown for a 40 kW, 3 km, 95% efficient aluminum conductor DC cable.

Figure 4 plots cable mass for a three-phase AC transmission cable. In this simplified example, the insulation thickness per peak voltage is maintained at an equal thickness to the DC case, however the higher peak voltage amplitude in an AC system requires thicker insulation for the same RMS voltage as compared to the DC case. This results in the AC cable being heavier than the DC cable.

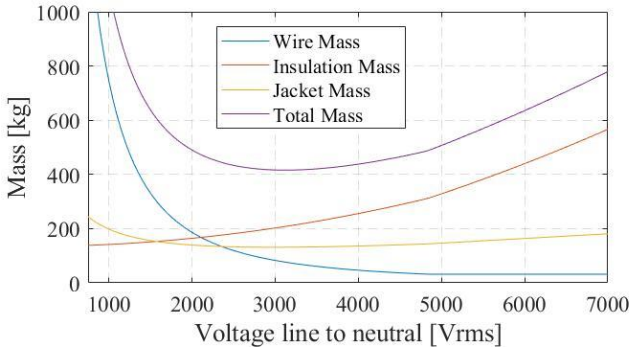

Figure 4: Mass breakdown for a 40 kW, 3 km, 95% efficient aluminum conductor three-phase AC cable.

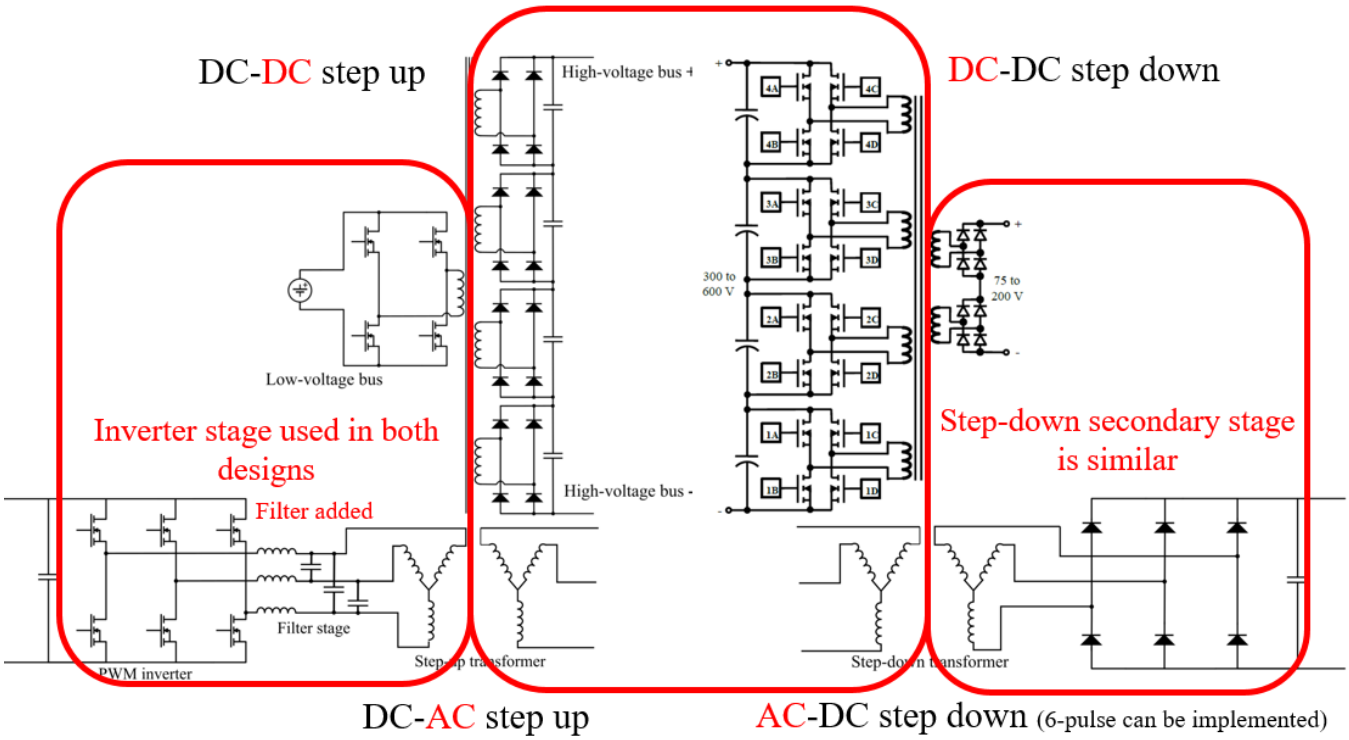

Figure 5: Comparison of topology for DC and AC transmission

It can also be noted that the AC system exhibits a minimum mass at a lower voltage than the DC case. In this example cable mass for the AC system is minimized at 3000 Vrms line-to-neutral or 5200 Vrms line-to-line. Based simply on cable mass estimates, a DC architecture appears to be advantageous, however the implementation of a DC system imposes challenges

IV. Voltage Boost Considerations

The implementation of electrical voltage boost for the lunar surface represents a significant challenge. At present, fully space qualified silicon devices are limited to 160 V operation. Progress is being made in the adoption of 650 V GaN devices, however single event effect radiation susceptibility is expected to limit their operating voltage significantly. To implement high-voltage power conversion using the available 160 VDC components, a stacked topology must be used if a DC transmission strategy is to be implemented.

One of the primary advantages of AC power during the development of terrestrial grids was the ability to use transformers to efficiently raise and lower voltages. While high voltage semiconductors have enabled processing high voltage DC power on earth, limitations in the availability of high-voltage radiation-tolerant devices forces a similar challenge on the lunar surface to that faced terrestrially.

IV.A Hardware implementation of AC vs. DC

Figure 5 is a comparison of a DC transmission architecture with an AC architecture under the assumption that both the lunar loads and sources are DC. This would hold for both PV and Stirling-based power generation. The regions outlined in red identify the three stages of conversion or transmission which occur in each system. In both systems the energy from the DC bus is converted to magnetic energy in the transformer. In the case of the DC system, a square-wave voltage in the 10s of kHz or higher in applied to the transformer primary. In the AC system, the 3-phase inverter is used to generate a 3-phase sinusoidal waveform using either a PWM or 6-step approach. This waveform is then filtered into a sinusoid using an LCL filter and fed into the primary winding of the 3-phase transformer.

The multiple secondary windings of the DC approach are each fed into full-wave rectifiers which rectify the square voltage waveform into a DC voltage with the aid of a filter capacitor at the output terminals. Each of the electrically isolated secondaries are connected in series to generate the intended DC distribution voltage. In the AC system, the transformer secondary is connected directly to the transmission lines without any further processing of the energy required.

The receiving, or step-down end of the DC power system is addressed with the auto-balancing series-stacked (ABSS) approach which has been demonstrated at GRC up to 600 V [23]. Additional work would be required to validate the ABSS stability and operation above 600 V. In the AC system, there is no inverter operation needed and

the incoming AC power is fed directly into the step-down transformer.

The secondary side of both the AC and DC step-down transformers are virtually identical. In both systems multiple secondaries with the appropriate turns ratio can be used to source a range of independent loads at different voltages. This arrangement will eliminate the need for the series stacking of multiple DC-DC converters to provide the full range of voltages needed for a habitat-type system. In the AC system, a 6-pulse delta/wye transformer configuration can also be implemented to minimize the capacitive filtering requirements at the load. In the DC system the capacitance required at the load is minimized because of the square output voltage waveform. Both topologies include the same number of electric to magnetic energy conversion steps however the AC approach removes the intermediate rectification and stacked H-bridges. Figure 5 demonstrates 4 stacked bridges. The number of bridges would grow as the transmission voltage divided by the voltage blocking capability of the individual switches. A 1 kV transmission voltage would require six stacked 175 V bridges.

Reliability is a critical aspect of any design intended for space applications. A detailed reliability calculation may be complex; however, the calculation of system failure rate is typically proportional to component count and a rough comparison of component count for AC and 1 kV DC topologies shows that the DC strategy requires approximately 4 times as many components in the power path and directly supporting it.

IV.B Additional Considerations

Past work has shown that DC and AC systems are expected to have comparable mass. AC was expected to have the best technology base and fewest development issues **[1]**. DC breakers are another technical challenge for DC systems. A DC breaker must extinguish the arc formed when interrupting current flow. This issue is not present in AC systems because the current flow is zero twice per cycle. High voltage DC breakers are an area of active research in the development of electric aircraft.

The synchronization and control of an AC grid with no spinning inertia will be more complex than a DC system, however AC system control is extremely well documented in literature and applied across the terrestrial power grid. General system stability in an inverter-based micro grid can be enhanced through synchronverter-style control which enables electronic inverters to emulate the rotational inertia of turbine-style generators. Under this strategy, standard droop-based control can be used to facilitate the coordination of multiple sources on the same AC system [24]. Corresponding strategies also exist for facilitating current sharing between parallel inverters which would allow parallel voltage-boost units to function independently without the complexity and development delay of a higher-level control system.

Work needs to be undertaken to understand the optimal frequency to use in the system, however, previous work has indicated that raising system transmission frequency has limited impact on the overall system mass because the power source mass dominates the overall mass [1]. As a reference point, single-phase 10 kW transformers designed for terrestrial 60 Hz applications are ~56 kg giving them a specific power density of 0.17 kW/kg [25] which is respectable considering that current NASA electric power conversion for flight missions falls in the range of 0.1 to 0.3 kW/kg. Additionally, it should be noted that increased losses resulting for high frequency skin effect in the transmission lines of an AC grid is not expected to be a challenge at the frequencies of interest. For reference, a 2 kHz sinusoid flowing in a 12 AWG wire will experience an increase in effective wire resistance of ~6%. This can be overcome by operating at a higher voltage or lower frequency as well as by using Litz wire.

In the AC approach, the transmission voltage is only limited by available insulation and can be adjusted depending on the distance energy is to be transmitted. Additionally, the AC transformer can potentially be arranged to act as radiation shielding for electronics. It should be noted that the use of AC power transmission for long-distance transmission does not automatically dictate an AC system throughout the lunar infrastructure. Because photovoltaic panels do not need extensive separation from the habitat, DC can be used for local power transfer.

V. Conclusions

This paper has reviewed some of the proposed strategies for lunar power transfer and discussed some of the benefits and design considerations of each. For low specific power nuclear power sources, maximizing the efficiency of power transfer is essential to minimizing the overall mass of the landed power system. At present, metallic conductors (copper or aluminum) offer the highest efficiency power transfer with the least programmatic risk for implementation. To minimize conductor mass, elevated AC or DC voltages will be required. An AC topology offers the possibility of a simplified architecture, while DC offers potentially simplified control implementation.

References

[1] K. J. Metcalf, R. B. Harty and J. F. Robin, "Issues concerning centralized versus decentralized power deployment," Rockwell International Corp.; Rocketdyne Div., Canoga Park, CA, 1991.

[2] C. B. Barth, D. M. Yang and M. F. Chaiken, "Design of a 1 kW, simplifed stirling controller

using capacitor-based power factor correction," in *Nuclear and Emerging Technologies for Space (NETS)*, Oak Ridge, TN, 2021.

[3] S. M. Geng, L. S. Mason, R. W. Dyson and L. B. Penswick, "Overview of multi-kilowatt free-piston Stirling power conversion research at Glenn Research Center," in *American Institute of Physics Conference Proceedings*, 2008.

[4] Teledyne e2v HiRel Electronics, "TDG650E15BEP Bottom-side cooled 650 V E-mode GaN FET," 2021.

[5] L. S. Mason, R. K. Shaltens, J. L. Dolce and R. L. Cataldo, "Status of Brayton cycle power conversion development at NASA GRC," in *AIP Conference Proceedings*, 2002.

[6] R. C. Evans, H. A. Klassen, C. H. Winzig and R. Y. Wong, "Evans, R. C., et al. Mechanical performance of a 2 to 10 kilowatt Brayton rotating unit.," Lewis Research Center, Cleveland, 1970.

[7] Staff of the Solar Dynamic Power Systems Branch, "Solar Dynamic Power System Development for Space Station Freedom," Lewis Research Center, Cleveland, OH, 1993.

[8] L. S. Mason, R. K. Shaltens and W. D. Espinosa, "Experimental Data for Two Different Alternator Configurations in a Solar Brayton Power System," 1997.

[9] L. Mason, A. Birchenough and L. Pinero, "Experimental Investigations From the Operation of a 2 kW Brayton Power Conversion Unit and a Xenon Ion Thruster," in *Space Technology and Applications International Forum*, Albuquerque, NM., 2004.

[10] D. Jenket, "Challenges for Power Beaming," in *Lunar Surface Innovation Consortium (LSIC) Power Beaming Workshop*, 2021.

[11] S. Ladan, S. Hemour and K. Wu, "Towards millimeter-wave high-efficiency rectification for wireless energy harvesting," in *2013 IEEE International Wireless Symposium (IWS)*, Beijing, 2013.

[12] D. E. Raible, "Free Space Optical Communications With High Intensity Laser Power Beaming," Cleveland, 2011.

[13] A. Wallace, G. Kushnir and R. Simpkin, *Verbal interview with Emrod*, Teams interview, 2022.

[14] M. Wagih, G. S. Hilton, A. S. Weddell and S. Beeby, "Millimeter-Wave Power Transmission for Compact and Large-Area Wearable IoT Devices Based on a Higher Order Mode Wearable Antenna," *IEEE Internet of Things Journal*, vol. 9, no. 7, pp. 5229-5239, 2022.

[15] MH GoPower Company Limited, "MH GoPower," 10 01 2021. [Online]. Available: http://www.mhgopower.com/images/Cell_Product_Brief_Rev_2.7_10-01-2021_EN.pdf. [Accessed 25 03 2022].

[16] "10 kW Nuclear Fission Power System," NASA Glenn Research Center Compass Lab, Cleveland, OH, 2020.

[17] M. Parks, C. Hayshi, K. Andrews, P. Jaffe, P. Jenkins, C. Cariste and T. Nugent, "Power Transmitted over Laser (PTROL) Point-to-point (P2P) Limited Operational Demonstration (LOD) Report," Naval Information Warfare Center Pacific, San Diego, California, 2020.

[18] B. Nugent, W. Johnson, M. Guzik and J. Stephens, "Space Exploration Applications for Development of High Capacity Cryocoolers," 2021.

[19] PHPK Technologies, "PHPK Technologies," 2005. [Online]. Available: http://www.PHPK.com. [Accessed 2022].

[20] D. S. Lashmore and P. Bystricky, *Manufacturing of High-Power Carbon Nanotube-based Cables - American Boronite Corp*, 2021.

[21] D. Lashmore, Interviewee, *Co-Founder & CEO of American Boronite Corp.*. [Interview]. 28th June 2021.

[22] D. Tsentalovich, Interviewee, *CEO, DexMat, Inc.* [Interview]. 7th June 2021.

[23] L. R. Pinero, K. E. Bozak, W. Santiago, R. J. Scheidegger and A. G. Birchenough, "Development of High-Power Hall Thruster Power Processing Units at NASA GRC," NASA Glenn Research Center, Cleveland, OH, 2015.

[24] Q.-C. Zhong and T. Hornik, Control of power inverters in renewable energy and smart grid integration, Chichester, West Sussex, PO19 8SQ, United Kingdom: John Wiley & Sons, Ltd, IEEE Press, 2013.

[25] Grainger Industrial Supply, "Single Phase Transformer Item #4WUE2," [Online]. Available: https://www.grainger.com. [Accessed 9 April 2020].